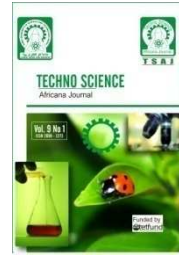




Techno Science Africana Journal

Journal homepage: www.technoscienceafricana.com



EFFECTS OF TRANSVERSE MODE SWITCHING AND GUIDING DYNAMICS IN LARGE AREA PHOTONIC CRYSTAL DEVICES

Yahaya Ado Sumaila

Department of Physics, Kano University of Science and Technology, P. M. B. 3244, Wudil, Kano-Nigeria.

ARTICLE INFO

Keywords:

carrier diffusion, mode partitioning, mode switching, near fields, photonic crystal, vertical-cavity lasers,.

Correspondence Author:

y_sumaila@yahoo.com,
+234 8056716228

ABSTRACT

This paper presents experimental investigation of the dynamics of mode partitioning and switching in a typical Photonics crystal laser device in the form of a vertical cavity surface emitting laser, VCSEL. The temporal evolution of the carrier density profile in a large area VCSEL is studied. Modal formation has been characterised in terms of switching times. Switching is observed at time scales associated with both the carrier diffusion and the thermal time constants. The dynamics have been observed from the nearfield patterns to have a slow build-up process and a fast switching speed.

INTRODUCTION

Unwanted excitation of modes at higher currents is one of the serious drawbacks of a photonic crystal surface emitting laser diode (PhC-SEL), thereby limiting their potential applications. In this paper, various modal formations are observed and their behaviour in terms of their switching times and stability are analysed which shows that there is need to investigate the manner and the formation speed of these multi-transverse modes in VCSEL devices. We investigate how modes form in time by measuring instantaneous near fields on nanosecond time scales. At the start, an overview is given of the modal noise in optical fibres and mode formation in conventional semiconductor lasers.

Mode partitioning in lightwave transmission systems can be an important factor causing system performance penalties and has been the subject of numerous experimental and theoretical studies [Linke *et al.*, (1985), Liu & Ogawa, (1984), Sasaki *et al.*, (1988), Ogawa (1982), Ohtsu & Teramachi, (1989), Cartledge & Elrefaie (1991), and Valle *et al.*, (1993)]. Such an investigation of intensity noise measurements has been reported in VCSELS

penalty is caused in part by several longitudinal modes experiencing differing dispersions in the optical fibre (Raddatz *et al.*, 1996). Random noise processes are responsible for the mode partitioning in semiconductor lasers. Mode partition may be one of the dominant performance limitations for the laser diode systems.

VCSELS have great roles to play in optical communication systems because of their inherent advantages such as high bit rate in multimode data links. However, there are several performance limitations in the utilisation of these devices, one of the more dominant being the mode partitioning noise, Kinichiro (1982), Vale and Pesquera (1994). This mode partition noise represents a major limitation in the performance of the devices; a large amount of work has been done on understanding guiding effects in VCSELS (Raddatz *et al.*, 1996) and (Sumaila, 1999). It has been shown that carrier induced anti-guiding plays an important role despite the presence of other guiding mechanisms (such as the carrier diffusion, strain etc.).

(Koyama *et al.*, 1991, Kutcha *et al.*, 1993 and Goobar *et al.*, 1995), but there has been no

single consideration on the dynamics of how the mode formation in these devices occurs. Therefore, visualising the dynamics of the mode formation in VCSELs would give interesting information on the relative importance of each effect. Observing the spatial behaviour of the lasing mode in time

and measuring the speed with which these modes switch would provide useful information.

Experimental Apparatus

The experimental apparatus (the InstaSpec-V ICCD system) used in this work are presented below in Fig. 1.

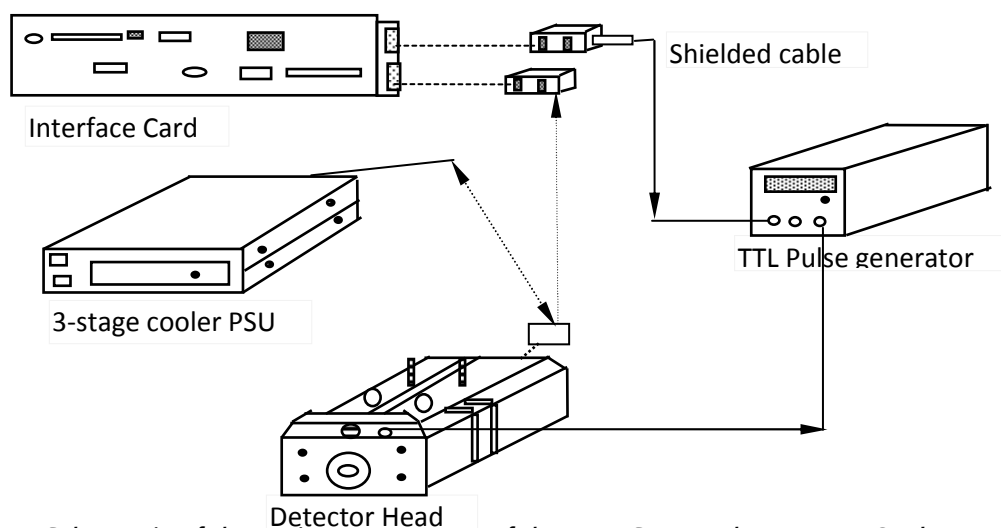


Figure 1: Schematic of the main components of the InstaSpec V Three stage Cooler system.

The InstaSpec V (Fig. 1), consists of several components such as:

- The detector Head
- Computer Interface Card
- Three Stage Cooler Power Supply Unit (PSU)
- Stanford Research System Delay Generator DG535

These components are briefly described in the following sections.

a. The Detector Head

The detector head contains the image intensifier and its gating electronics, the charged-coupled device (CCD) sensor and its pre-amplifier, Fig. 2. It also contains the temperature sensor, the sensor's pre-amplifier and the thermoelectric cooler. The head is attached to the interface card via a shielded cable for acquiring data.

Inside the detector head, the head is in a hermetically sealed housing that has been flushed with dry gas, and hence there is no need to be concerned about condensation when the head is cooled to below the dew point temperature if water-cooling system is used. In our own case we used the electric cooling system. The thermoelectric cooling greatly enhances the performance of the InstaSpec ICCDs. The operations of some major parts of the ICCD are given in the section below.

b. The Three Stage Power Supply Unit (PSU) Cooler

The detector head of the InstaSpec-V system has a 3 stage thermoelectric cooler model which allows the system to operate at lower temperature. This system requires a lot of power and hence, a separate power supply unit is used to power the system, as shown in Fig. 1.

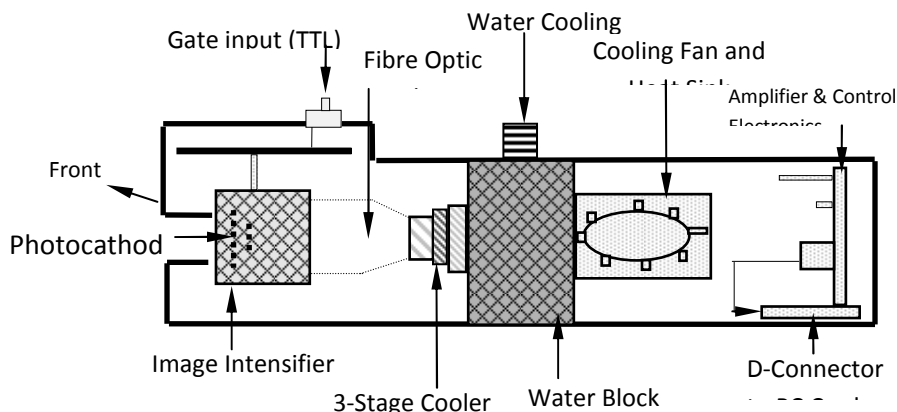


Figure 2: Schematic of the ICCD-camera Head [Oriel Instruments, (1996)]

c. Stanford Research System Delay Generator DG535/01

The Stanford Research System (SRS) delay generator model DG535/01 is used for setting up this system and is used to produce the transistor-transistor logic (TTL) pulses needed to operate the intensifier gating electronics situated in the detector head. In order to get a

complete image, a high repetition rate pulse is required, and a typical timing diagram is shown in Fig. 3. The pulse generator is controlled by computer through a graphical processor interface board (GPIB) connection that sends the pulse to the laser as well as to the detector head simultaneously.

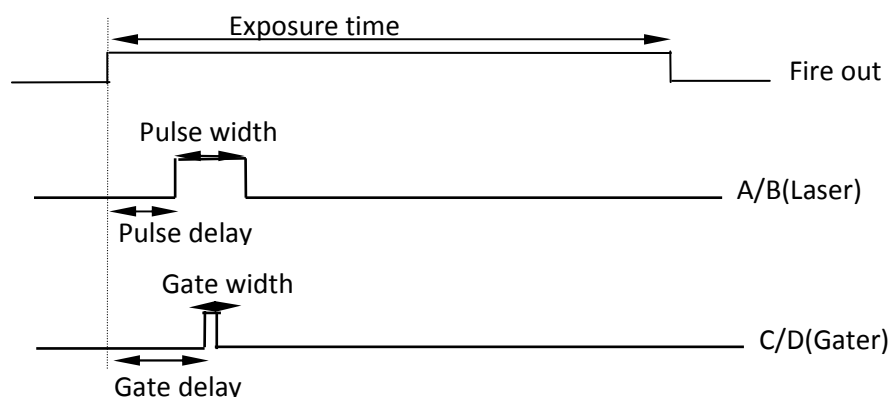


Figure 3: Schematic of the timing diagram of the SRS delay generator.

EXPERIMENTAL METHODOLOGY

Figure 4 shows the experimental arrangements used in this work. The VCSEL used in the set-up is a 15µm gain guided top-emitting GaAs QW device grown by gas source molecular beam epitaxy, (Hahn *et al.*, 1993). It consists of 23 pairs of top DBR mirrors and 32.5 pairs of bottom DBR mirror. The current confinement has been due to the proton implantation, which guided the carriers in the

active region of the device. The laser oscillates at a wavelength of 840 nm and has a threshold current is 7 mA. The photodiode used is a large area Silicon Avalanche (Si-APD) with a diameter of 100 µm operated at a dc-bias voltage of 180 V. This is important as this much lower temperature preserves the detector as well as reducing noise in the measured results.

The camera shutter is chosen to open after a variable delay, and the time for data acquisition is fixed here at the minimum value of 5ns. In order to align the detector head and

the laser beam, a linear image sensor mode (LIS) is chosen and several runs are done until a good alignment is attained. A variable attenuator is used to avoid camera saturation.

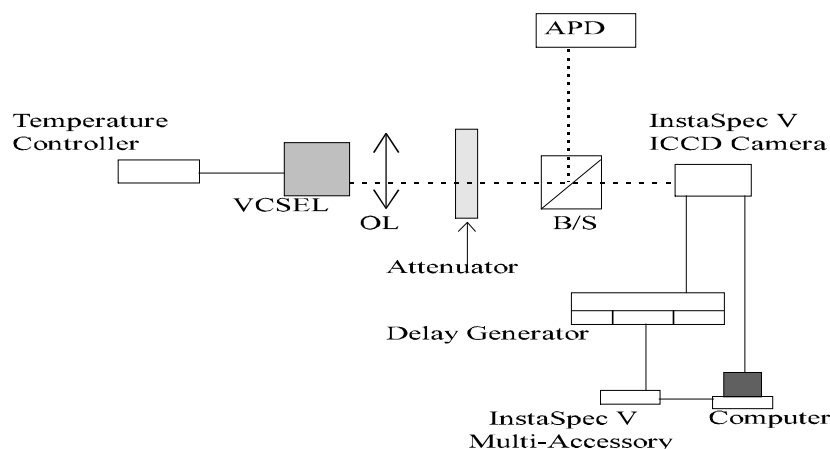


Figure 4: Schematic for the experimental set-up; OL is a microscope objective lenses, B/S is beam-splitter.

Near Field Measurement

The near field measurements are obtained by driving the VCSEL at sub-threshold currents and an ICCD camera with a high-speed shutter is used to record the near field images. This image is observed by imaging the spontaneous emission of the device onto the CCD. The recording sequences of the camera have been highlighted in the previous sections. Both the camera and the VCSEL are operated under the InstaSpec-V software control. The gate delay is varied so that the image of the near field can be displayed in time with a time delay accuracy of a few nanoseconds. A 5 μs pulse width is applied to the laser using the delay generator with a pulse delay of 1 μs and the camera gate is kept constant at just 5ns. The bias current to the laser is fixed for each particular measurement. The near field of the VCSEL is measured by changing the delay to the camera’s gate and scans the laser beam by sampling a point in time across.

Each image consists of 256 vertical pixels and 1023 horizontal pixels. Therefore, the camera has to open its shutter 256 times to scan a single image and this takes a minimum of 25 ms. This time of 25 ms is known as the camera’s exposure time.

Real time measurements have been carried out to determine the spatial effects measured

by the camera. These give the real time power measurements as detected by the Si-APD. Because the diameter of the magnified laser beam is larger (approximately 2 mm) than that of the photodiode, it is possible for power measurement of the VCSEL to be plotted as a function of time at different positions of its facet. Results obtained from these measurements are given in Fig. 6.

RESULTS AND DISCUSSION

The results of the time-resolved near-field measurements and the real time power measurements described above are presented here.

i. Mode Partitioning Effect

Figure 5 shows some near field patterns which exhibit mode partitioning. This is very similar to the results found by (Sumaila Y. 2013). The mode partitioning of the steady state near field also depends on the value of the bias current applied to the VCSEL. It can be seen that at a bias of 13mA, the modes in the device cavity spread outwards in the form of a ring shape. The image is grey-scaled with the darkest regions corresponding to the highest intensities. In Fig. 5 (b), the region of low intensity (indicated by white area), is a hole at the center of the mode that is deprived of carriers due to spatial hole burning generated in the laser cavity.

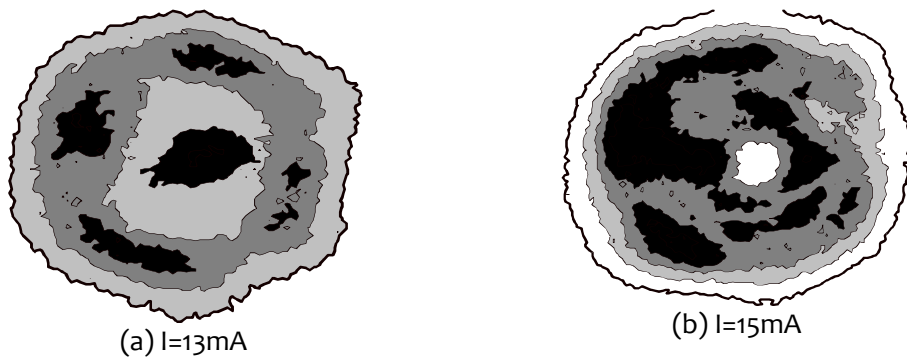


Figure 5: Steady state near-field patterns for bias currents of (a) 13mA and (b) 15mA.

From Fig. 5 (a), if the current is increased above 13 mA, the near-field moves in a clockwise direction and the light distribution across the facet of the VCSEL becomes more complex as shown in Fig.5 (b). This is known as mode partitioning. This complexity can be explained in terms of thermal lensing effects. At higher current, around 15 mA a hole appears in the emission at the central region surrounded by a

near circular intensity profile. The mode distribution later settles down with higher currents but still with circular near field shape. Fig. 6 shows that the power emitted from the device stabilises after about 1.5 μ s. The laser is pre-biased at a sub-threshold (5 mA) before applying 13 mA and 15 mA and peak amplitude of 4.5 μ s pulses

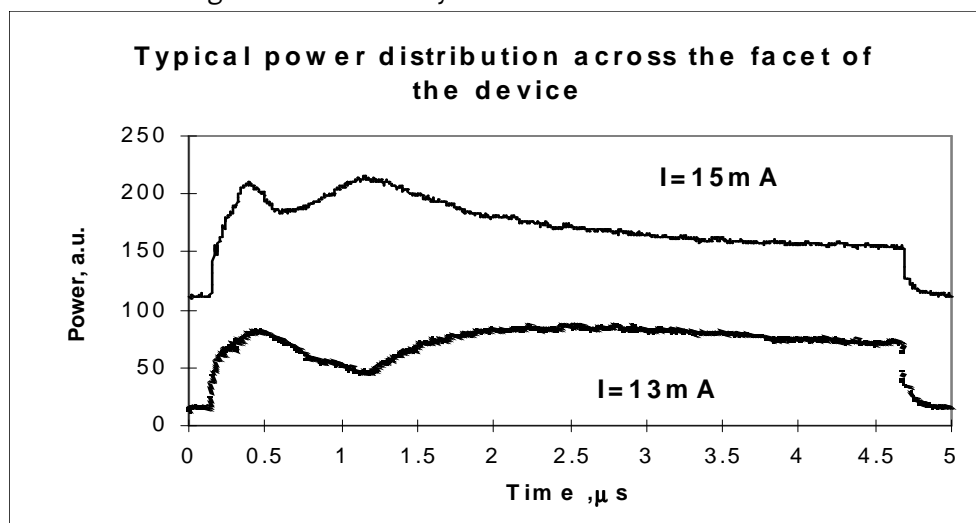


Figure 6: Si-APD response showing the total power of the mode partition development due to optical filaments.

Plots in Fig. 6, shows the variation of power from the spatial regions, which changes considerably until stabilisation on long time scales (several microseconds). The figure shows the total power of the mode partition development due to optical filaments, at dc-bias

5mA and pulse current of 13mA and 15mA. The carrier density distribution across the device has also been measured from the spontaneous emission spectra. This gives the information on the carrier distribution in the device.

ii. Mode Stabilisation time

Mode partitioning observed as in Fig. 7 shows that at this dc-bias of 15mA during the laser turn-on the mode starts to form in one side of the device’s cavity, spreads out later becoming circular with a low intensity area in the middle. Figure 8 shows the variation of the stabilisation time plotted with changing bias currents. From this figure (Fig. 8), it can also be observed that

the stabilisation time without any pre-bias current is always longer than with any offset pre-bias current. Mignosi *et. al.*,(1996) have found similar behaviour with the devices they used. The greater the offset current, the faster the stabilisation is attained. The stable state of the mode formation is also observed to be achieved more quickly with the combination of higher dc offsets and higher bias currents.

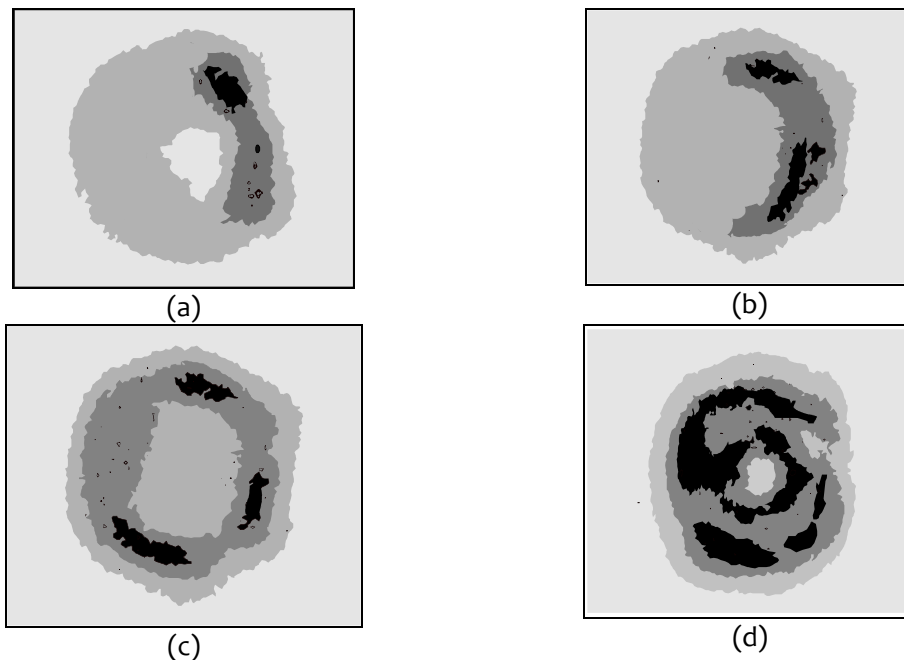


Figure 7 Formation of optical filaments due to carrier guiding and mode partitioning at I=15 mA, (a) 30 ns, (b) 50 ns, (c) 250 ns, (d) 3μs.

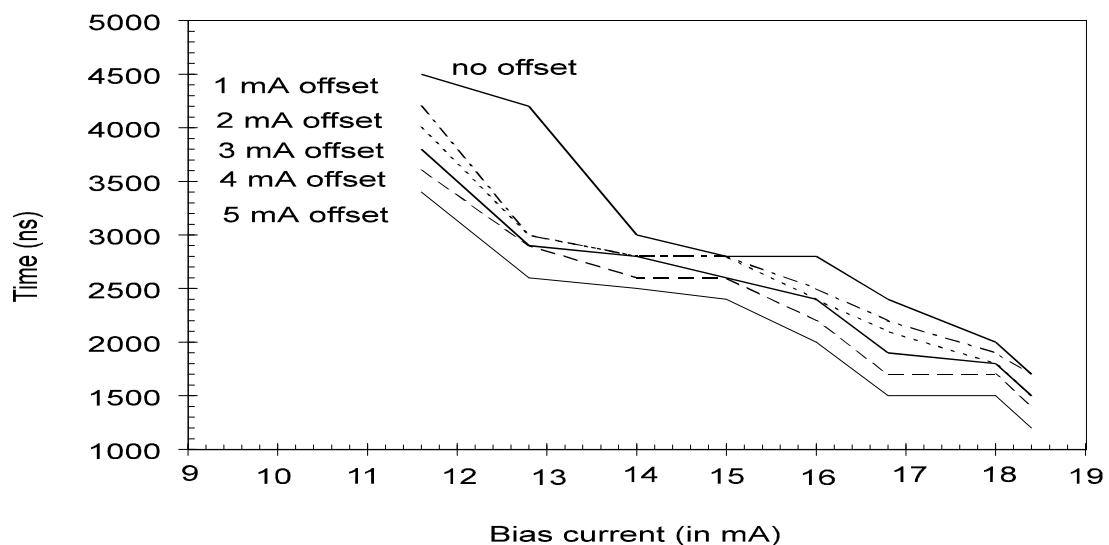


Figure 8: Time required in attaining stable state versus dc-bias currents.

DISCUSSIONS AND CONCLUSION

The first measurements of the dynamics of transverse mode partitioning and switching have been studied from a 15 μm GaAs QW VCSELs using an InstaSpec-V ICCD systems and a large area Si-APD. The measurements have shown that modes forming in this device are complex and vary in time and with applied dc-bias currents. Two mechanisms have been observed to be associated with this, carrier diffusion and thermal effects. The dynamics have been observed to have a slow build-up process and a fast switching speed (Figs. 7 and 8). Under pulsed condition, carriers are injected nearly all over the surface of the device and reach stable state within very few nanoseconds of the pulse turn-on. The path of the

partitioning is believed to be guided by thermal effects, Mignosi and Sumaila (2013) and Sumaila (2016) which indeed depends on the dc-bias currents applied to the VCSEL as well as on the carrier density. The higher concentration of carriers implies that a stable state is attained more quickly. The carrier diffusion times is found to be within 20 ns but can be as long as 100 ns, while the thermal time scales are found to be appreciably longer (up to 1 μs or 2 μs). Single peaks are found to be dominant at the beginning of the pulse ($\sim 0 - 1000$ ns or more), after which several peaks appear and later form a ring shape with a hole at the centre of the mode. This exhibits the spatial hole-burning phenomenon of the mode partitioning in large area VCSEL devices.

REFERENCES

- Cartledge J. C. and Elrefaie A. F., (1991), "Threshold gain difference requirements for nearly single longitudinal mode lasers," *IEEE J. Lightwave Technol.*, Vol. 9, pp. 809-811.
- Goobar E., Scott J. W., Thibeault B., Robinson G., Akulova Y., and Coldren L., (1995), "Calibrated intensity noise measurements in microcavity laser diodes," *Appl. Phys. Lett.*, Vol. 67, pp. 3697-3699.
- Hahn K. H., Tan M. R., Houngh Y. M., and Wang S. Y., (1993), "Large area Multi-transverse-mode VCSELs for modal noise reduction in multimode fibre systems," *Electron. Lett.*, Vol. 29, pp. 1482-1483.
- InstaSpec Instruction Manual, for ICCD Detector, *Oriel Instruments*, (1996), Model 77193-5 pp. 28.
- Kinichiro O., (1982), "Measurements of mode partition noise of laser diodes," *IEEE J. Quantum Electron.*, Vol. QE-18, pp. 1090-1093.
- Koyama F., Morito K., and Iga K., (1991), "Intensity noise and polarisation stability of GaAlAs surface emitting lasers," *IEEE J. Quantum Electron.*, Vol. 27, pp. 1410-1416.
- Kutchka D. M., Gamelin J., Walker J. D., Lin J., Lau K. Y., and Smith J. S., (1993), "Relative intensity noise of vertical cavity surface emitting lasers," *Appl. Phys. Lett.*, Vol. 62, pp. 1194-1197.
- Linke R. A., Kasper B. L., Burrus C. A., Jr., Kaminov I. P., Ko J. S. and Lee T. P., (1985), "Mode power partition events in nearly single frequency lasers," *IEEE J. Lightwave Technol.*, Vol. LT-3, pp. 706-712.
- Liu P. -L. and Ogawa K., (1984), "Statistical measurements as a way to study mode partition in injection lasers," *IEEE J. Lightwave Technol.*, Vol. LT-2, pp. 44-48.
- Marcuse, D. (1985), "Computer simulations of laser photon fluctuations: DFB lasers," *IEEE J. Quantum Electron.*, Vol. QE-21, pp. 161-167.
- Mignosi C., Sumaila Y., Dowd P. and White I., "Dynamics of Mode Partitioning in Vertical Cavity Surface Emitting Lasers", A Report Submitted to the Centre for Communications Research, University of Bristol, UK., and to the Hewlett Packard Laboratories, USA, July-Oct., 1996.

- Ogawa K., (1982), "Analysis of mode partition noise in lasers transmission systems," *IEEE J. Quantum Electron.*, Vol. QE-18, pp. 849-855.
- Ohtsu M., and Teramachi Y., (1989), "Analyses of mode partition and mode hopping in semiconductor lasers," *IEEE J. Quantum Electron.*, Vol. QE-25, pp. 31-38.
- Raddatz L., White I. H. and Summers H. D., (1996), "Measurements of guiding effects in vertical cavity surface emitting lasers," *IEEE Photon Technol. Lett.*, Vol. 8, pp. 743-745.
- Sasaki S., Choy M. M. and Cheung N. K., (1988), "Effects of dynamic spectral mode behaviour and mode partition of DFB lasers on Gbit/s transmission systems," *IEEE J. Quantum Electron.*, Vol. 24, pp. 26-28.
- Sumaila (2013), "Transverse Mode Partitioning in Vertical Cavity Surface Emitting Lasers (VCSELs), Proceedings of the 1st-International Conference on Research and Sustainable Development, Keffi, Nasarawa State, Nigeria, 5th - 8th Feb. 2013.
- Sumaila, Y. (1999), PhD Thesis, University of Bristol, UK.
- Vale A. and Pesquera L., (1994), "Mode Partition noise in multi-transverse vertical-cavity surface-emitting lasers", Instituto de Fisica de Cantabria (CSIC-Universidad de Cantabria) Facultad de Ciencias, Avda, Los Castros s/n E 39005, Santander Spain, 1994.
- Valle A., Colet P., Pesquera L. and San Miguel M., (1993), "Transient multimode statistics in almost single mode semiconductor lasers," *IEEE Proc. J. Opto-electron.*, Vol. 140, pp. 237-242.